A Novel External Immobilization Method to Establish a Rat Model of Knee Extension Contracture

Yun Zhou (zhouyunanhui@sina.com)
The Second Hospital of Anhui Medical University
Chen Xu Zhou
The Second Hospital of Anhui Medical University
Feng Wang
The Second Hospital of Anhui Medical University
Wang Hua
2. Key Laboratory of Environmental Toxicology of Anhui Higher Education Institutes
Qiao Zhou Fang
The Second Clinical Medicine College of Anhui Medical University
Kai Ge Xiong
The Second Clinical Medicine College of Anhui Medical University
Quan Bing Zhang
The Second Hospital of Anhui Medical University

Research Article

Keywords: joint external immobilization,extending knee joint contracture, myogenic contracture, arthrogenic contracture

Posted Date: March 11th, 2022

DOI: https://doi.org/10.21203/rs.3.rs-1434993/v1

Abstract

Background: The study aimed to elucidate the formation process and therapeutic strategies of knee extension contracture, we developed a novel rat model using an aluminum external fixator.

Methods: Sixty male SD rats with mature bones were divided into the control group (n=6) and groups that had the left knee immobilized with an aluminum external fixator for 1, 2, and 3 days, and 1, 2, 3, 4, 6, and 8 weeks (n=6 in each group). The passive extension range of motion, histology, and expression of fibrosis-related proteins were compared between the control group and the immobilization groups.

Results: Myogenic contracture progressed very quickly during the initial 2 weeks of immobilization; after 2 weeks, the contracture gradually changed from myogenic to arthrogenic. The arthrogenic contracture progressed slowly during the first week, rapidly progressed until the third week, and then showed a steady progression. Histological analysis confirmed that the anterior joint capsule of the extended fixed knee became increasingly thicker over time. Correspondingly, the level of TGFβ-1 in the anterior joint capsule also increased with the immobilization time. Over time, the cross-sectional area of muscle fibers gradually decreased, while the amount of intermuscular collagen and TGFβ-1 increased. Unexpectedly, the amount of intermuscular collagen and TGFβ-1 decreased during the late stage of immobilization (6–8 weeks).

Conclusion: Myogenic contracture is stabilized after 2 weeks of immobilization, while arthrogenic contracture is stabilized after 3 weeks of immobilization. This novel rat model may be a useful tool to study the etiology of joint contracture and establish new therapeutic approaches.

Background

Knee contracture is currently one of the most common clinical diseases and is characterized by joint capsule fibrosis and a restricted range of activity secondary to periarticular intermuscular connective tissue hyperplasia [1]. The signature pathology of joint contracture is the proliferation of myofibroblasts (active fibroblasts) and the deposition of proteins in the extracellular matrix in the joint capsule and intermuscular connective tissue [2]. The most common cause of knee contracture is prolonged immobilization, which is clinically used as an acute treatment for musculoskeletal disease to relieve knee pain and reduce inflammation [3,4]. Knee contracture is unsightly and has adverse effects on function and quality of life, affecting daily activities such as ascending and descending stairs, walking, and toileting. Furthermore, knee contracture is very difficult to treat [5]. Despite a large amount of rehabilitation, conservative treatment, and even surgical treatment, it is difficult to completely restore the joint mobility, and this loss of mobility seriously decreases the quality of life of patients and adversely affects the distribution of medical resources in society [6,7]. It is therefore very important to investigate the mechanisms leading to knee contracture.

The contracture mechanism has been explored in many studies. As early as 1993, a rat flexion contracture model was successfully established by fixing the tibia and fibula in complete flexion (150°)

for up to 7 weeks without damaging the joints [8]. In recent years, various immobilization methods have been introduced to create flexion contracture models by fixing the animal knee joint at about 150° of flexion, including hook buckle (a hook-and-loop fastener) immobilization [9] and helix (spiral wire) immobilization [10]. In contrast, extension contracture models are rare. However, the extension contracture model is of clinical relevance because it better mimics fracture and bed-associated immobilization than the flexion contracture model.

According to the general international standard, the neutral position of the knee joint is the straightened or extended position, which is defined as 0°. The functional position of the knee joint is from 15° to 20° of flexion, while the range of motion (ROM) of the normal knee is 120° to 150° for flexion and 5° to 10° for overextension. Knee injury usually requires immobilization in a straightened or functional position, but this type of immobilization may result in limited knee flexion activity (knee extension contracture); therefore, knee extension contracture is the most common type of knee contracture. It is critical to study knee extension contracture using appropriate animal models; however, the current literature describes several animal knee contracture models, most of which involve flexion knee contracture. Thus, it is necessary to establish a convenient and reliable rat model of knee extension contracture.

In the present study, we aimed to explore the process of knee joint contracture formation during immobilization by creating a novel rat model of knee extension contracture by externally fixing the knee in a straightened position. To our knowledge, this is the first report of a rat model of knee extension contracture.

Methods

Establishment of a rat model of knee extension contracture

Male SD rats (age 6–8 weeks) were obtained from our experimental animal center and used in this experiment. Aluminum splints (6061; Longkai, Suzhou, China), sponge (33d, Changzhou, China), and woodworking (BND-2815, Bonida, Guangdong, China) were prepared. The rats were kept under the same conditions without intervention for 2 weeks before the experiment (free diet, day and night balance, temperature 20–25℃, humidity 50% ± 5%). Each rat was placed on the operating table in the supine position and fixed as shown in Figure 1. Immobilization was performed under general anesthesia achieved with an intraperitoneal injection of 10% chloral hydrate (0.03 ml/kg). A patent application has been made for the self-made aluminum splint (patent number: 202120470158.0).

Measurements of the knee joints of 8-week-old male rats (n=15) revealed that the average thigh width was 3.23±0.21 cm (range 6.38±0.41 to 7.21±0.43 cm) and the average calf width was 4.86±0.27 cm (range 2.34±0.13 to 5.11±0.36 cm). In accordance with the anatomical characteristics of the rats, the novel immobilization device was fixed with an aluminum plate and bonded with a 0.5-cm-thick sponge on the skin to prevent excessive immobilization. The shape of the aluminum plate is shown in Figure 1A–B.

The novel fixation device placed the knee joint in the straightened position and ensured complete external immobilization of the knee joint.

Grouping and specimen collection

Sixty rats were randomly divided into 10 groups (n=6 in each group). The control group had no intervention, while the immobilization groups had the left hindlimb fixed for 1 day (immobilization-1d group), 2 days (immobilization-2d group), 3 days (immobilization-3d group), 1 week (immobilization-1w group), 2 weeks (immobilization-2w group), 3 weeks (immobilization-3w group), 4 weeks (immobilization-4w group), 6 weeks (immobilization-6w group), and 8 weeks (immobilization-8w group). At each timepoint, the rats in the appropriate group were euthanized by an excessive intraperitoneal injection of 10% chloral hydrate. After euthanasia, the fixed left hindlimb of the rat was removed at the hip joint. The skin was separated, and the knee mobility was measured using the measurement device designed for this experiment (Figure 2). The muscles were then separated. The rectus femoris was divided into two parts; one part was frozen at 80℃ for protein molecular weight detection, while the other part was fixed in 4% paraformaldehyde for Sirius red staining. Knee mobility was measured after the separation of the muscles. The anterior joint capsule was divided into two parts; one part was frozen at 80℃ for protein molecular weight detection, while the other part was fixed in 4% paraformaldehyde for hematoxylin and eosin (HE) staining. During the experiment, the rats were free to move within the cage with the immobilization device attached.

Measurement of joint mobility

A joint mobility meter was used to measure the joint activity of the left knee of 10 SD rats (Figure 3A–B). The cruzi needle was penetrated from the femoral neck parallel to the femur. Fixed ture pin pin by magnetic suction removable metal clamp. The distal tibia was secured to the turntable with disposable plastic ties. The digital force gauge was secured to the slide. On the base of the equipment was a rope attached to the groove of the turntable and a digital dynamometer. The turntable moved when the drive wheel was turned to indirectly turn the tibia while the femur was stationary. The applied force was displayed on the screen of the digital force meter, and the angular change between the femur and tibia (the disk radius, the force arm) was constant and was calculated according to the scale of the turntable. Therefore, the force moment and the force size showed a linear relationship. The moment size and the angle also had a corresponding relationship. The applied torque was calculated by multiplying the force by the constant radius of the disk. Knee ROM was measured with 5.3 N-cm as the standard torque. This torque brings the knee close to its physiological limit [11] but does not damage the soft tissue [12,13]. The mobility of each left knee was measured three times by two researchers, giving six measurements. The knee ROM before and after myotomy was measured to yield the total, myogenic, and arthrogenic contracture using a previously described method [14]. (1) Degree of total contracture = ROM before myotomy (knee joint in the control group) - ROM before myotomy (knee joint in the immobilization group);

(2) degree of arthrogenic contracture = ROM after myotomy (knee joint in the control group) - ROM after myotomy (knee joint in the immobilization group); (3) degree of myogenic contracture = degree of total contracture - degree of arthrogenic contracture.

Histological evaluation

Specimens used for joint mobility assessment were used to evaluate the histology of the knee joint. After the ROM measurements, the left rectus femoris and anterior knee joint capsule were fixed in 4% paraformaldehyde (pH 7.4) at 4°C for approximately 36 hours. The specimens were embedded in paraffin. The rectus femoris specimens were cut into 5-μm coronal sections, while the joint capsule specimens were sectioned into 5-μm sagittal sections.

Sirius red staining

Rectus femoris sections were stained with Sirius red solution for 1 hour (2610-10-8; Solarbio Life Science, Beijing, China) and rinsed with running water to remove the surface dye. Nuclei were stained with Mayer's hematoxylin solution for 8 to 10 minutes and flushed with running water for 10 minutes. Sections were then conventionally dehydrated and sealed with neutral gum. The muscle collagen fiber density and muscle fiber cross-sectional area for each region were assessed using ImageJ software version 1.53a (National Institutes of Health, Bethesda, Maryland, USA, available at https://imagej.nih.gov/ij/). Histological analysis was performed on six rats in each group, with three slides for each rat.

HE staining

The joint capsule sections were stained with HE using the following steps. (1) Paraffin sections were dewaxed and then placed in xylene I for 10 minutes, xylene for 10 minutes, anhydrous ethanol I for 5 minutes, anhydrous ethanol for 5 minutes, 95% alcohol for 5 minutes, 90% alcohol for 5 minutes, 80% alcohol for 5 minutes, 70% alcohol for 5 minutes, and finally washed with distilled water. (2) Sections were stained with Harris hematoxylin for 3–8 minutes, rinsed with tap water and differentiated with 1% ethanol hydrochloride for several seconds, and then rinsed with tap water again. The sections were returned to blue with 0.6% ammonia and rinsed with running water. (3) Sections were stained in eosin solution for 1–3 minutes. (4) To attain the dehydration seal, the sections were placed in 95% alcohol I for 5 minutes, 95% alcohol II for 5 minutes, anhydrous ethanol I for 5 minutes, anhydrous ethanol II for 5 minutes, xylene I for 5 minutes, and xylene II for 5 minutes; the sections were then removed from the xylene to dry and were sealed with neutral gum. (5) Microscopic examination, image acquisition, and histological analysis were performed on six rats in each group, with three slides for each rat.

Proteomics analysis of muscle and joint capsule

Protein immunoblotting (western blotting) was performed as follows. Total protein was extracted from the retained muscle and joint capsule samples. When 50–60 mg of rectus femoris muscle was taken, the total tissue protein was extracted with 600 ml of RIPA reagent (Tris-HCl (pH 7.4), 150 mmol/L NaCl, 1 mmol/L EDTA, 1% Triton X-100, 1% sodium deoxycholate, 0.1% SDS, and 1 mmol/L P MSF), and a protease inhibitor was added to the RIPA. Total proteins were separated by SDS-PAGE and transferred to the PVDF membrane. The Sirius red staining was cut to the appropriate size and washed and immersed in 5% skim milk for 4℃ overnight. Membranes were incubated with anti-rat monoclonal transforming growth factor beta-1 (TGFβ-1) antibody (1:10,000–50,000, Cell Signaling, USA) for 2 hours at room temperature, and then washed three times with a TBST solution containing 0.1% Tween-20 (10 minutes/wash). The washed PVDF membrane was incubated with horseradish peroxidase-labeled goat anti-rat IgG antibody (1:10,000–50,000, Cell Signaling, USA) for 1 to 2 hours at room temperature, washed with TBST (as described above), and then detected with ECL light-emitting liquid colored with energy autoexposure. The developing bands were analyzed by IPP software and quantified with GAPDH as an internal reference. The expression of TGFβ-1 protein was examined.

Statistical analysis

The results are expressed as the mean ± standard deviation (SD). One-way analysis of variance was used to test the difference between groups. $P < 0.05$ indicated significant differences. Statistical analyses were performed using IBM SPSS Statistics software, version 22 (IBM Corp., Armonk, NY, USA).

Results

Three rats in the immobilization-6w group experienced slippage of the immobilization device in the second week of immobilization; the immobilization device was fixed on the same day as the slippage occurred, and there was no further slippage until the end of the immobilization period. There was no death, lower limb necrosis, or other complications in any group.

Joint activity

Total contracture

After 1 week of immobilization, the degree of total contracture significantly differed between the control group and the immobilization groups (all $P < 0.05$). Compared with the immobilization-1d, -2d, and -3d groups, the degree of total contracture was significantly greater in the immobilization-1w, -2w, -3w, -4w, -6w, and -8w groups (all $P < 0.05$). The degree of total contracture did not significantly differ between adjacent immobilization groups, i.e., between the immobilization-1d and -2d, immobilization-2d and -3d, immobilization-3w and -4w, immobilization-4w and -6w, and immobilization-6w and -8w groups. The degree of total contracture increased with the immobilization time (Table 1).

Table 1

Total, myogenic, and arthrogenic contracture after knee immobilization for various time periods in 60 SD rats (mean ± SD)

Grouping	Quantity	Degree of contracture(°)		
		Total contracture	Myogenic contracture	Arthrogenic contracture
Control	6	0.0±0.0	0.0±0.0	0.0±0.0
Immobilization-1d	6	1.1±0.6	0.6±0.4	0.5±0.3
Immobilization-2d	6	2.4±0.7	1.5±0.4	0.9±0.2
Immobilization-3d	6	5.9±1.0	4.0±1.0	1.9±0.5
Immobilization-1w	6	23.5±2.0[abcd]	15.9±1.9[abcd]	7.6±0.7[abcd]
Immobilization-2w	6	51.8±1.8[abcde]	32.7±1.1[abcde]	19.1±1.3[abcde]
Immobilization-3w	6	78.7±2.2[abcdef]	33.9±2.1[abcde]	44.5±1.9[abcdef]
Immobilization-4w	6	79.9±2.8[abcdef]	34.2±2.2[abcde]	44.9±2.2[abcdef]
Immobilization-6w	6	80.8±3.5[abcdef]	35.5±2.9[abcde]	45.3±2.9[abcdef]
Immobilization-8w	6	82.5±3.0[abcdef]	35.9±2.5[abcde]	46.6±2.3[abcdef]

[a]$P < 0.05$ vs control group; [b]$P < 0.05$ vs immobilization-1d group; [c]$P < 0.05$ vs immobilization-2d group; [d]$P < 0.05$ vs immobilization-3d group; [e]$P < 0.05$ vs immobilization-1w group; [f]$P < 0.05$ vs immobilization-2w group.

Myogenic contracture

The degree of myogenic contracture was significantly greater in the immobilization-1w group than the immobilization-3d group ($P < 0.05$). The degree of myogenic contracture also significantly differed between the immobilization-1w and -2w groups ($P < 0.05$), but not between any other adjacent immobilization groups ($P > 0.05$). The results suggested that myogenic contracture occurred after 1 week of immobilization and gradually stabilized after 2 weeks of immobilization, while the subsequent joint contractures were mostly arthrogenic (Table 1).

Arthrogenic contracture

After 1 week of immobilization, the degree of arthrogenic contracture was significantly greater in the immobilization groups than the control group ($P < 0.05$). The degree of arthrogenic contracture significantly differed between the immobilization-3d and -1w, immobilization-1w and -2w, and immobilization-2w and -3w groups (all $P < 0.05$), but not between the other adjacent groups ($P > 0.05$). The results suggested that arthrogenic contracture progressed from 1 to 3 weeks of immobilization. However, the progression amplitude of the arthrogenic contracture began to weaken after 3 weeks of immobilization (Table 1).

Histological evaluation of the Sirius red-stained sections

In comparison with the control group, the mean diameter of the rectus femoris significantly decreased with the duration of immobilization in all immobilization groups except the immobilization-1d and -2d groups ($P < 0.05$). From 1 day to 3 weeks of immobilization, the proportion of collagen fibers in the rectus femoris of the immobilization groups increased with the fixation time. The proportion of collagen fibers significantly differed between the control group and all immobilization groups except the immobilization-1d, -2d, and -3d groups ($P < 0.05$). The proportion of collagen fibers in the rectus femoris stabilized in the immobilization-4w group, but was decreased in the immobilization-6w and -8w groups ($P < 0.05$ in all cases, Figure 4).

Histological evaluation of the hematoxylin-eosin-stained sections

The largest synovial area in the sagittal plane was analyzed. HE staining showed that the degree of synovial hyperplasia of the anterior joint capsule in the immobilization groups increased with the fixation time, with significant differences between adjacent groups, i.e., between the immobilization-1d and -2d, immobilization-3d and -1w, immobilization-1w and -2w, and immobilization-2w and -3w groups ($P < 0.05$). The degree of synovial hyperplasia of the anterior joint capsule also significantly differed between the control group and all immobilization groups, except the immobilization-1d group ($P < 0.05$, Figure 5).

Protein expression in muscle and joint capsule

After early joint immobilization, the expression level of TGF-β1 significantly increased in the joint capsule and muscles. The expression level of TGF-β1 in the joint capsule was significantly higher in the immobilization-1w group than the immobilization-3d group. TGF-β1 expression of joint capsule continued to increase after immobilization for up to 8 weeks. There were significant differences in TGF-β1 levels in the joint capsule between the immobilization-2d and -3d, immobilization-1w and -2w, and immobilization-2w and -3w groups ($P < 0.05$). The TGF-β1 content of the anterior joint capsule increased with the immobilization time, with a slight downward trend in the immobilization-8w group that did not reach statistical significance ($P > 0.05$). TGF-β1 expression in the anterior joint capsule was significantly

increased in the control group compared with the immobilization groups ($P < 0.05$), except the immobilization-1d and -2d groups. Western blot results showed that the TGF-β1 content in the quadriceps muscle first increased and then decreased. The TGF-β1 content in the muscle significantly differed between the immobilization-2d and -3d, immobilization-3d and -1w, immobilization-1w and -2w, and immobilization-6w and -8w groups ($P < 0.05$); significant differences were also found between control group and immobilization groups ($P < 0.05$), except the immobilization-1d and -2d groups (Figure 6).

Discussion

Joint contracture is a relatively common condition that is mainly caused by fibrosis of the joint capsule and skeletal muscle after long-term immobilization, and shows the pathological features of excessive deposition of collagen and connective tissue components [15]. Numerous animal models have been developed to simulate knee flexion contracture; however, few animal models of knee extension contracture have been reported. A previous study successfully established a model of knee extension contracture in New Zealand white rabbits [16] and reported in detail the characteristics of plaster immobilization and the relevant mechanisms. However, it is beneficial to model knee extension contracture in rats rather than rabbits because of the lower cost of studying the pathogenesis of joint contracture and evaluating therapeutic efficacy. Therefore, the present study described a method to establish a novel model of knee extension contracture in the rat. We demonstrated that this novel model had significantly limited knee flexion activity and altered expressions of histological and fibrosis-related proteins in the skeletal muscle and anterior joint capsule.

The biological findings of this study showed that the degree of total contracture was significantly greater in the immobilization-1w group than the control group, but did not significantly differ between the immobilization-4w and immobilization-3w groups; this indicates that the knee flexion activity was significantly after 1 week of immobilization and stabilized after 3 weeks of immobilization. The degree of myogenic contracture was significantly greater in the immobilization-1w group than the control group, but did not significantly differ between the immobilization-2w and immobilization-3w groups; this indicates that myogenic contracture began to develop after 1 week of immobilization and stabilized after 2 weeks of immobilization. The degree of arthrogenic contracture was significantly greater in the immobilization-1w group than the control group, but did not significantly differ between the immobilization-3w and immobilization-4w groups; this indicates that arthrogenic contracture began to develop after 1 week of immobilization and stabilized after 3 weeks of immobilization.

Oki et al. [17] directly assessed the muscle limitations of rats with immobilized ankle joints and found that the initial flexion contracture of the knee is mainly due to muscle structure and is reversible and can spontaneously resolve. In contrast, long-term contracture is mainly caused by the joint structure and is irreversible [14]; such arthrogenic contracture cannot be improved, even by aggressive rehabilitation [18]. Several reports suggest that joint contractures occur within 1 week of immobilization and progress in a time-dependent manner [19,20]. Chimoto et al. [21] reported that 2 weeks of muscle limitation mainly causes myogenic contracture, while long-term contracture (more than 4 weeks of immobilization) results

in joint contracture. Therefore, prolonged immobilization for longer than 4 weeks should be avoided to prevent irreversible joint contracture [22]. In the present study, myogenic contracture was the predominant type of contracture during the first 2 weeks of immobilization. From 2 to 3 weeks of immobilization, the joint contracture changed from myogenic to arthrogenic. The contracture initiation time in the present study was consistent with previous studies; however, in contrast with previous studies, the arthrogenic contracture stabilized at 3 weeks. Arthrogenic contracture is primarily a fibrotic response within the joint capsule. The posterior joint capsule is the main contributor to the formation of immobilization-induced knee flexion contracture [23], while the anterior joint capsule has the greatest impact on knee extension contracture. The synovial layer of the anterior joint capsule is the widest and most complex in the knee joint [24]. In the present study, the degree of synovial hyperplasia continuously increased with the immobilization time; this may explain why knee extension contracture forms earlier than knee flexion contracture.

In the histologic assessment of the present study, the myofiber cross-sectional area, intermuscular collagen deposition, and extent of hyperplasia in the anterior joint capsule supported the biological findings. The myofiber cross-sectional area was significantly smaller in the immobilization-3d group than the control group, not in group immobilization-3w, after 3 days after 2 weeks of immobilization, as the decreased skeletal muscle mass caused by an imbalance in protein metabolism is characterized by a significantly smaller muscle fiber area [25,26,27]. The amount of intermuscular collagen deposition was significantly greater in the immobilization-1w group than the control group, but did not significantly differ between the immobilization-2w and − 3w groups. Furthermore, there was significantly less intermuscular collagen deposition in the immobilization-6w group compared with the immobilization-4w group. This indicates that intermuscular collagen deposition began to increase in the first week of immobilization, but decreased after 4 weeks of immobilization. Previous studies have shown that this may be associated with gradual resolution of the inflammatory and fibrotic response after immobilization [11]. This was demonstrated by the reduction in collagen content and TGF-β1 protein expression over time. The anterior joint synovial proliferation was significantly greater in the immobilization-2d group than the control group, but did not differ between the immobilization-3w and − 4w groups, indicating that the anterior joint synovial proliferation significantly increased during the first 3 weeks of immobilization and stabilized from 3 weeks onwards. Takemura et al. [28] analyzed changes in the synovial membrane caused by anterior articular capsule fibroblasts, microvasodilation, and congestion due to plaster immobilization. Watanabe et al. [29] and Matsuzaki et al. [30] reported that intra-articular tissue adhesion does not completely cover the cruciate ligament in and around the knee, but originates from synovial fibrosis. The proliferation of intra-articular synovial tissue was responsible for the limited ROM found in the present study.

To further characterize the altered fibrosis of skeletal muscle and the joint capsule, we evaluated the expression of the TGF-β1 protein. TGF-β1 is the most important cytokine during fibrosis because it promotes the differentiation of fibroblasts into myofibroblasts, myofibroblast proliferation, and the production of collagen [31]. The aggravation of contracture enhances the fibrosis response, characterized by increases in profibrotic genes and proteins (such as cytokine TGF-β1 genes, type I and type III collagen

genes and proteins), leading to increases in collagen density and joint capsule thickness [32]. Hildebrand et al. [33] reported increased expressions of type I and III collagen and TGF-β1 in a rabbit post-traumatic flexion contracture model compared with control joint cysts. The increased mRNA levels of TGF-β1 may be related to collagen deposition inside and outside of the articular capsule. Joint capsule fibrosis may be associated with the development of joint contracture. Similarly, the present study showed that the expression of fibrosis-related genes increased with prolonged immobilization, but the TGF-β1 expression in the rectus femoris decreased slightly after 3 weeks of immobilization and was significantly decreased at 8 weeks. The altered expression levels of TGF-β1 may be due to hypoxia or a reduction in collagen turnover or degradation rates [34]. Among several other roles, one of the adaptive responses of hypoxic cells is the upregulation of hypoxia-inducible factor 1 alpha (HIF-1α). The expressions of TGF-β1 and HIF-1α are significantly upregulated during the transformation of fibroblasts to myofibroblasts [35], leading to the promotion of vascular endothelial growth factor (VEGF) gene expression. The HIF-1α signaling pathway in turn regulates angiogenesis by inducing VEGF expression, thereby improving circulation and reducing the inflammatory response [36].

In the present study, ordinary gypsum and polymer gypsum were initially used to establish the extended knee contracture model. However, the rats inevitably gnawed the gypsum and there was also gypsum slippage. In the process of switching to an aluminum splint, we found that the knee joints of the rats could not be wrapped when fixed because the proximal lower limbs were short and strong. The present shape of the external immobilization device was determined after multiple improvements. The immobilization device comprised of aluminum plate pressurized at the distal end on the back of the foot that was plantarflexed at 60°. After the first proximal rectangular aluminum plate was used to fix the knee joint, the second inverted trapezoidal aluminum plate was wrapped around the knee to ensure that the knee was completely immobilized. Although this novel immobilization method is simple, the pressure strength must be carefully controlled. A pressure that is too high will easily cause poor limb circulation in rats. As aluminum is easy to shape, we were able to adjust the tightness of the external immobilization to resolve any swelling. Kotaro et al. [37] successfully created a model of flexion contracture outside the knee joint; however, the external immobilization device used in the present study had less effect on the overall activity of the rats and better reflected the clinical situation in which the knee joint is usually fixed in extension after injury, leading to limited knee flexion after long-term immobilization. Therefore, to more closely mimic the clinical situation, we chose to create a model of knee extension contracture.

We demonstrated that the present model is as reliable as other animal models in reproducing the features of human joint contracture, including limited joint mobility, changes in the joint and muscle histology, and changes in the expression of fibrosis-associated proteins in the joint capsule versus muscle. The advantage of the present model is that it is easy to replicate because it does not require complex surgical procedures, the tools are easy to use, and the rat anesthesia and immobilization can be performed in a very short period of time. We described the detailed process of establishing a rat model of knee extension contracture, with photographs. The model closely replicates joint contracture caused by complications of immobilization, enabling researchers to investigate the etiology of joint contracture and establish new treatments. This model is a reliable tool that can be used to study the prevention and treatment of knee

extension contracture in rats, while making it possible to change the dressing and keep the wound dry during immobilization of traumatic knee contracture.

The present study had some limitations. First, in this model, the ankle joint and the knee joint were inevitably fixed together. Because the lower limb of the rat is shaped like a cone, the ankle joint was plantarflexed at 60° and fixed with the knee joint to prevent slippage of the aluminum splint. Second, the longest immobilization time in the present study was 8 weeks. We plan to explore the continuous longer-term changes in fibrosis-related proteins in a future study. Finally, the formation time of the arthrogenic contracture of the extended knee joint was different from that reported for knee flexion contracture; however, the present study only evaluated the protein expression and histological findings.

Conclusions

The results in this study suggested that myogenic contracture was stabilized after 2 weeks, while arthrogenic contracture was stabilized after 3 weeks. This novel rat model may be a useful tool to study the etiology of joint contracture and establish new therapeutic approaches.

Abbreviations

ROM, range of motion

HE staining, hematoxylin and eosin staining

TGFβ-1, transforming growth factor beta-1

HIF-1α , hypoxia-inducible factor (HIF)-1alpha

VEGF, vascular endothelial growth factor

Declarations

Ethics approval and consent to participate

All experimental procedures were performed in accordance with the Guidelines for Animal Experimentation of Anhui Medical University and were approved by the Institutional Animal Care and Use Committee of Anhui Medical University (LLSC20190761).

Consent for publication

Not applicable.

Availability of data and material

The datasets used and analysed during the current study are available from the corresponding author on reasonable request.

Authors' contributions

Chen Xu Zhou conceived the study, participated in its design and coordination and drafted the manuscript. *Feng Wang* participated in the design of the study and performed the statistical analysis. *Yun Zhou* and *Wang Hua* participated in its design and coordination, and helped to draft the manuscript. *Qiao Zhou Fang and Kai Ge Xiong* drew the pictures in the manuscript. *Quan Bing Zhang* performed the statistical analysis in the revised manuscript. All authors read and approved the final manuscript.

Competing interests

The authors declare that they have no competing interests.

Funding

This study was supported by Clinical Medicine Discipline Construction Project of Anhui Medical University in 2021 (2021LCXK031), Anhui Key Research and Development Program (201904a07020067), Anhui Medical University Clinical Medicine Discipline Construction Project Clinical and Preliminary Co-construction Discipline Project (amu202210), Provincial quality project of Higher education in Anhui Province (2020jyxm0903) and Anhui Medical University Research Foundation (2018xkj050).

Acknowledgements

We thank Professor *Hua Wang* from School of Public Health, Anhui Medical University for his valuable corrections and advice.

Contributor Information

Chen Xu Zhou, Email: 754087439@qq.com

Feng Wang, Email: 987035340@qq.com

Yun Zhou, Email: zhouyunanhui@sina.com

Wang Hua, Email: wanghuadev@126.com

Qiao Zhou Fang, Email: 919778166@qq.com

Kai Ge Xiong, Email: 1913230090@stu.ahmu.edu.cn

Quan Bing Zhang , Email: quanbingzhang@126.com

References

1. Sato Y, Ono T, Ishikura H, Aihara K, Tasaka A, Umei N, Tsumiyama W, Oki S. The recovery time required for rat joint contractures treated with joint fixation with unweighting of the hind limbs. J Phys Ther Sci. 2019;31(4):336-339. doi: 10.1589/jpts.31.336.
2. Hinz B, Lagares D. Evasion of apoptosis by myofibroblasts: a hallmark of fibrotic diseases. Nat Rev Rheumatol. 2020;16(1):11-31. doi: 10.1038/s41584-019-0324-5.
3. Winston BA, Jones J, Ries MD. Flexion contracture due to cyclops lesion after bicruciate-retaining total knee arthroplasty. Arthroplast Today. 2019;5(4):442-445. doi: 10.1016/j.artd.2019.09.003.
4. Zhang QB, Zhou Y, Zhong HZ, Liu Y. Effect of Stretching Combined With Ultrashort Wave Diathermy on Joint Function and Its Possible Mechanism in a Rabbit Knee Contracture Model. Am J Phys Med Rehabil. 2018;97(5):357-363. doi: 10.1097/PHM.0000000000000873.
5. Zhuang Z, Yu D, Chen Z, Liu D, Yuan G, Yirong N, Sun L, Liu Y, He R, Wang K. Curcumin Inhibits Joint Contracture through PTEN Demethylation and Targeting PI3K/Akt/mTOR Pathway in Myofibroblasts from Human Joint Capsule. Evid Based Complement Alternat Med. 2019;2019:4301238. doi: 10.1155/2019/4301238.
6. Yu D, Zhuang Z, Ren J, Hu X, Wang Z, Zhang J, Luo Y, Wang K, He R, Wang Y. Hyaluronic acid-curcumin conjugate suppresses the fibrotic functions of myofibroblasts from contractive joint by the PTGER2 demethylation. Regen Biomater. 2019;6(5):269-277. doi: 10.1093/rb/rbz016.
7. Wang F, Zhang QB, Zhou Y, Chen S, Huang PP, Liu Y, Xu YH. The mechanisms and treatments of muscular pathological changes in immobilization-induced joint contracture: A literature review. Chin J Traumatol. 2019;22(2):93-98. doi: 10.1016/j.cjtee.2019.02.001.
8. Akai M, Shirasaki Y, Tateishi T. Viscoelastic properties of stiff joints: a new approach in analyzing joint contracture. Biomed Mater Eng. 1993;3(2):67-73.
9. Onda A, Kono H, Jiao Q, Akimoto T, Miyamoto T, Sawada Y, Suzuki K, Kusakari Y, Minamisawa S, Fukubayashi T. New mouse model of skeletal muscle atrophy using spiral wire immobilization. Muscle Nerve. 2016;54(4):788-91. doi: 10.1002/mus.25202.
10. Aihara M, Hirose N, Katsuta W, Saito F, Maruyama H, Hagiwara H. A new model of skeletal muscle atrophy induced by immobilization using a hook-and-loop fastener in mice. J Phys Ther Sci. 2017;29(10):1779-1783. doi: 10.1589/jpts.29.1779.
11. Kaneguchi A, Ozawa J, Minamimoto K, Yamaoka K. Formation process of joint contracture after anterior cruciate ligament reconstruction in rats. J Orthop Res. 2021;39(5):1082-1092. doi: 10.1002/jor.24800.
12. Trudel G, Uhthoff HK. Contractures secondary to immobility: is the restriction articular or muscular? An experimental longitudinal study in the rat knee. Arch Phys Med Rehabil. 2000;81(1):6-13. doi:

10.1016/s0003-9993(00)90213-2.

13. Moriyama H, Yoshimura O, Sunahori H, Tobimatsu Y. Comparison of muscular and articular factors in the progression of contractures after spinal cord injury in rats. Spinal Cord. 2006;44(3):174-81. doi: 10.1038/sj.sc.3101802.
14. Trudel G, Laneuville O, Coletta E, Goudreau L, Uhthoff HK. Quantitative and temporal differential recovery of articular and muscular limitations of knee joint contractures; results in a rat model. J Appl Physiol (1985). 2014;117(7):730-7. doi: 10.1152/japplphysiol.00409.2014.
15. Le Sant G, Nordez A, Andrade R, Hug F, Freitas S, Gross R. Stiffness mapping of lower leg muscles during passive dorsiflexion. J Anat. 2017;230(5):639-650. doi: 10.1111/joa.12589.
16. Zhou Y, Zhang QB, Zhong HZ, Liu Y, Li J, Lv H, Jing JH. Rabbit Model of Extending Knee Joint Contracture: Progression of Joint Motion Restriction and Subsequent Joint Capsule Changes after Immobilization. J Knee Surg. 2020;33(1):15-21. doi: 10.1055/s-0038-1676502.
17. Oki S, Ono T, Shimizu ME, Otsuka A, Kanai S. Contribution of articular and muscular structures to the limitation of rangeof motion after joint immobility: an experimental study on the rat ankle. Biomedical Research. 2008;19(2): 78-81.
18. Xu QY, Zhang QB, Zhou Y, Liu AY, Wang F. Preventive effect and possible mechanisms of ultrashort wave diathermy on myogenic contracture in a rabbit model. Sci Prog. 2021;104(4):368504211054992. doi: 10.1177/00368504211054992.
19. Nagai M, Aoyama T, Ito A, Iijima H, Yamaguchi S, Tajino J, Zhang X, Akiyama H, Kuroki H. Contributions of biarticular myogenic components to the limitation of the range of motion after immobilization of rat knee joint. BMC Musculoskelet Disord. 2014;15:224. doi: 10.1186/1471-2474-15-224.
20. Trudel G, Uhthoff HK, Goudreau L, Laneuville O. Quantitative analysis of the reversibility of knee flexion contractures with time: an experimental study using the rat model. BMC Musculoskelet Disord. 2014;15:338. doi: 10.1186/1471-2474-15-338.
21. Chimoto E, Hagiwara Y, Ando A, Itoi E. Progression of an arthrogenic motion restriction after immobilization in a rat experimental knee model. Ups J Med Sci. 2007;112(3):347-55. doi: 10.3109/2000-1967-207.
22. Kaneguchi A, Ozawa J, Kawamata S, Yamaoka K. Development of arthrogenic joint contracture as a result of pathological changes in remobilized rat knees. J Orthop Res. 2017;35(7):1414-1423. doi: 10.1002/jor.23419.
23. Chimoto E, Hagiwara Y, Ando A, Itoi E. Progression of an arthrogenic motion restriction after immobilization in a rat experimental knee model. Ups J Med Sci. 2007;112(3):347-55. doi: 10.3109/2000-1967-207.
24. Zhao X, Meng F, Hu S, Yang Z, Huang H, Pang R, Wen X, Kang Y, Zhang Z. The Synovium Attenuates Cartilage Degeneration in KOA through Activation of the Smad2/3-Runx1 Cascade and Chondrogenesis-related miRNAs. Mol Ther Nucleic Acids. 2020;22:832-845. doi: 10.1016/j.omtn.2020.10.004.

25. Wang F, Zhang QB, Zhou Y, Liu AY, Huang PP, Liu Y. Effect of ultrashort wave treatment on joint dysfunction and muscle atrophy in a rabbit model of extending knee joint contracture: Enhanced expression of myogenic differentiation. Knee. 2020;27(3):795-802. doi: 10.1016/j.knee.2020.02.013.
26. Jin SB, Tian ZB, Ding XL, Guo YJ, Mao T, Yu YN, Wang KX, Jing X. The Impact of Preoperative Sarcopenia on Survival Prognosis in Patients Receiving Neoadjuvant Therapy for Esophageal Cancer: A Systematic Review and Meta-Analysis. Front Oncol. 2021;11:619592. doi: 10.3389/fonc.2021.619592.
27. Wang F, Li W, Zhou Y, Huang PP, Zhang QB. Radial extracorporeal shock wave reduces myogenic contracture and muscle atrophy via inhibiting NF-κB/HIF-1α signaling pathway in rabbit. Connect Tissue Res. 2021 May 20:1-10. doi: 10.1080/03008207.2021.1920934.
28. Takemura K, Hoso M, Yoshikubo H. Histopathological Effects of the Stretching on Joint Components after Two-week Knee Joint Immobiliza-tion in Rats. Rigakuryohogaku. 2004; 31: 76-85.
29. Watanabe M, Hoso M, Takemura K, Yoshikubo H, Matsuzaki T, Kojima S. Histopathological changes in joint components during contracture -A study of the long term knee joint immobility model in the rat. Rigakuryoho Kagaku. 2007;22(1): 67-75.
30. Matsuzaki T, Kojima S, Watanabe M, , Yoshida S, Hoso M. Histopathological changes in the infrapatellar fat-pad of rats with knee contracture. Ishikawa Journal of Physical Therapy. 2012; 12: 11-14 .
31. Kaneguchi A, Ozawa J, Minamimoto K, Yamaoka K. Active exercise on immobilization-induced contractured rat knees develops arthrogenic joint contracture with pathological changes. J Appl Physiol (1985). 2018;124(2):291-301. doi: 10.1152/japplphysiol.00438.2017.
32. Kaneguchi A, Ozawa J, Minamimoto K, Yamaoka K. Low-Level Laser Therapy Prevents Treadmill Exercise-Induced Progression of Arthrogenic Joint Contracture Via Attenuation of Inflammation and Fibrosis in Remobilized Rat Knees. Inflammation. 2019;42(3):857-873. doi: 10.1007/s10753-018-0941-1.
33. Hildebrand KA, Zhang M, Germscheid NM, Wang C, Hart DA. Cellular, matrix, and growth factor components of the joint capsule are modified early in the process of posttraumatic contracture formation in a rabbit model. Acta Orthop. 2008;79(1):116-25. doi: 10.1080/17453670710014860.
34. Hagiwara Y, Ando A, Onoda Y, Matsui H, Chimoto E, Suda H, Itoi E. Expression patterns of collagen types I and III in the capsule of a rat knee contracture model. J Orthop Res. 2010;28(3):315-21. doi: 10.1002/jor.20997.
35. Huang PP, Zhang QB, Zhou Y, Liu AY, Wang F, Xu QY, Yang F. Effect of Radial Extracorporeal Shock Wave Combined With Ultrashort Wave Diathermy on Fibrosis and Contracture of Muscle. Am J Phys Med Rehabil. 2021;100(7):643-650. doi: 10.1097/PHM.0000000000001599.
36. Zimmermann SM, Würgler-Hauri CC, Wanner GA, Simmen HP, Werner CM. Echinomycin in the prevention of heterotopic ossification - an experimental antibiotic agent shows promising results in a murine model. Injury. 2013;44(4):570-5. doi: 10.1016/j.injury.2012.12.030.

37. Tokuda K, Yamanaka Y, Kosugi K, Nishimura H, Okada Y, Tsukamoto M, Tajima T, Suzuki H, Kawasaki M, Uchida S, Nakamura E, Wang KY, Sakai A. Development of a novel knee contracture mouse model by immobilization using external fixation. Connect Tissue Res. 2022;63(2):169-182. doi: 10.1080/03008207.2021.1892088.

Figures

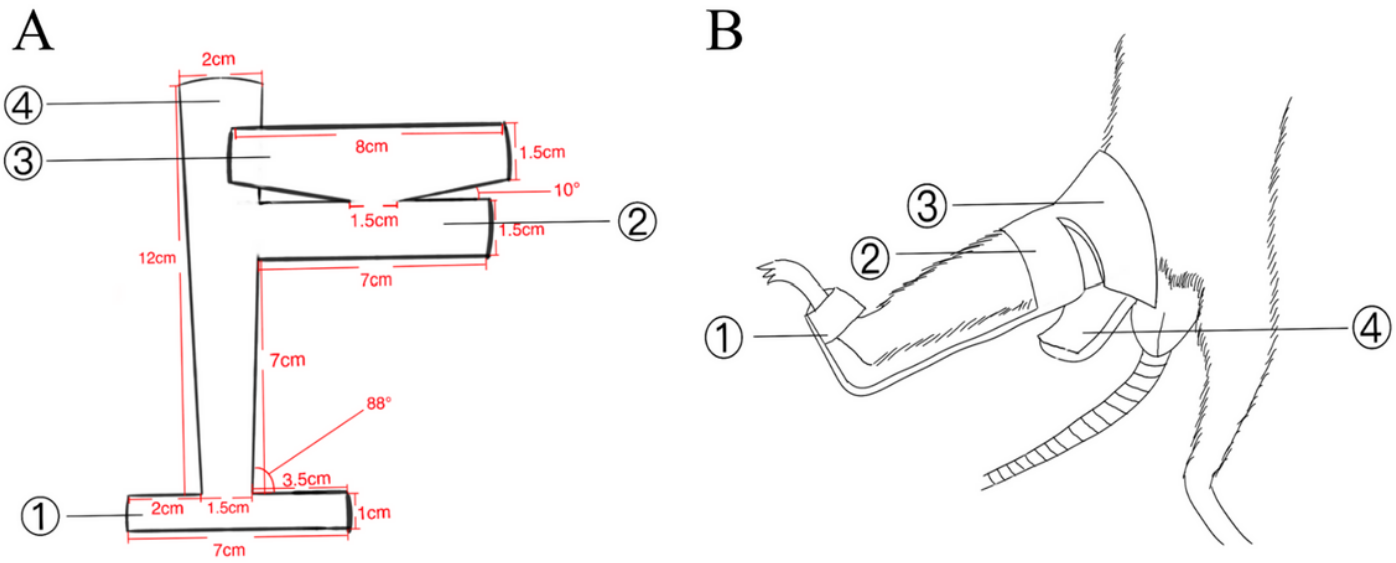

Figure 1

A: Schematic diagram of the aluminum splint attached to a rat. ① The back of the distal foot is fixed to prevent the lower limb from slipping through the immobilization device. ② The periphery of the knee joint is fixed. ③ As the rat knee is shaped like an inverted conical structure, this design aims to fix the distal end of the rat femur. ④ A fulcrum is created by appropriate bending of the splint under the rat femur. B: Schematic diagram of the immobilization device.

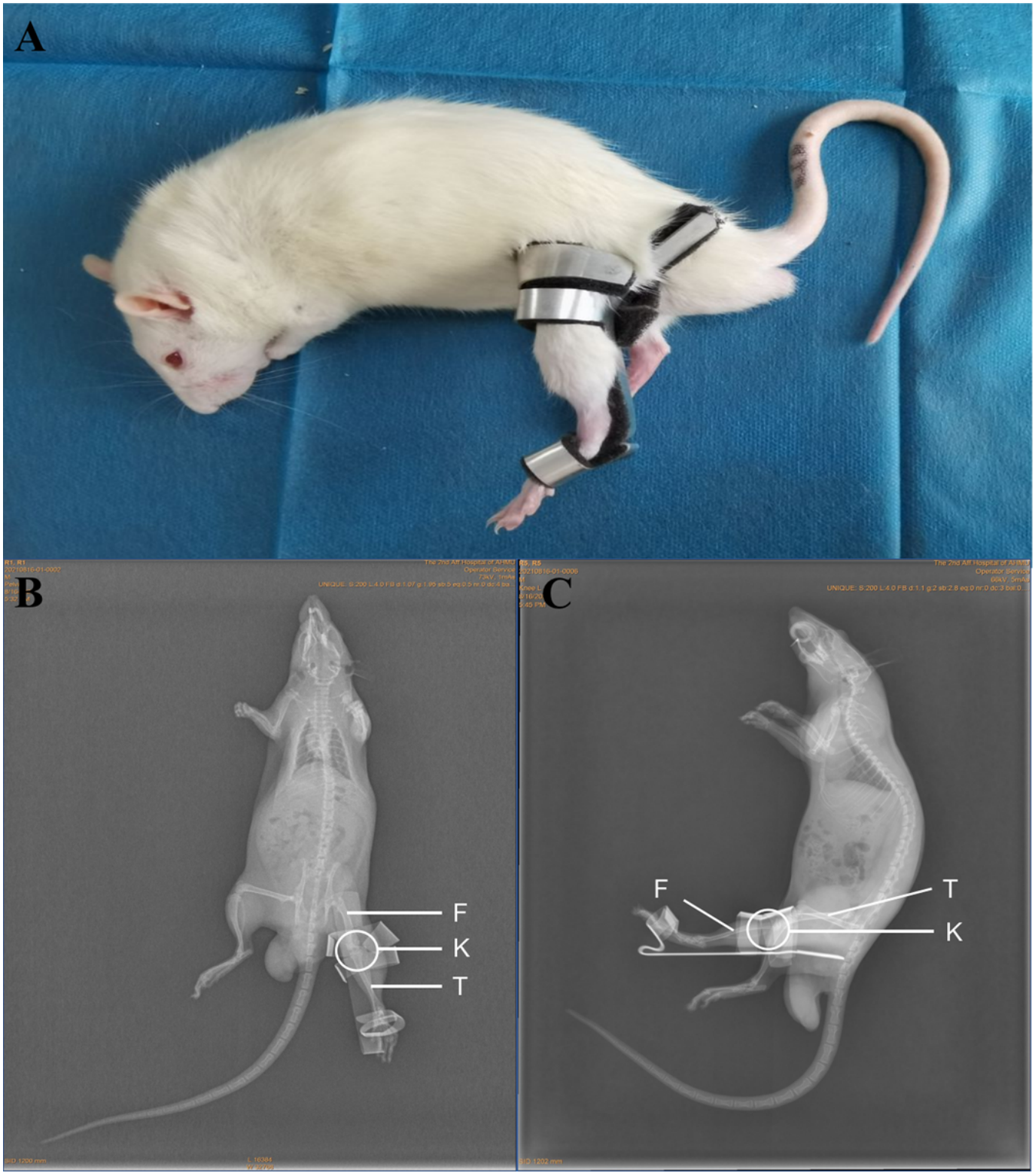

Figure 2

A: Photograph of a rat with the left knee immobilized. B: Orthotopic radiograph of the rat knee joint after immobilization. C: Lateral radiograph of the rat knee joint after immobilization. F, femur; K, knee; T, tibia.

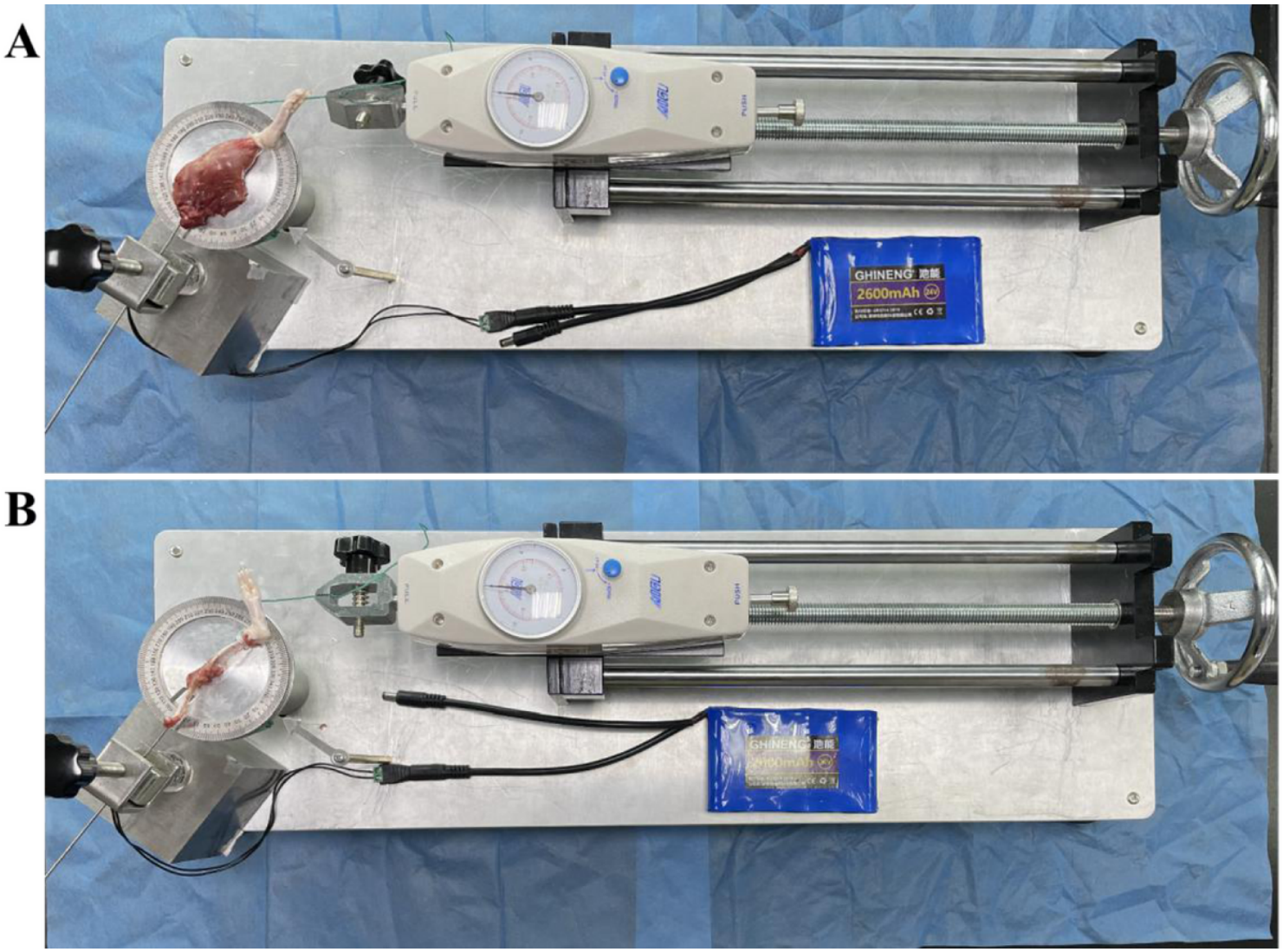

Figure 3

A: Schematic diagram of peeling activity (total contracture) measurement. B: Schematic representation of the activity measured after muscle separation (arthrogenic contracture).

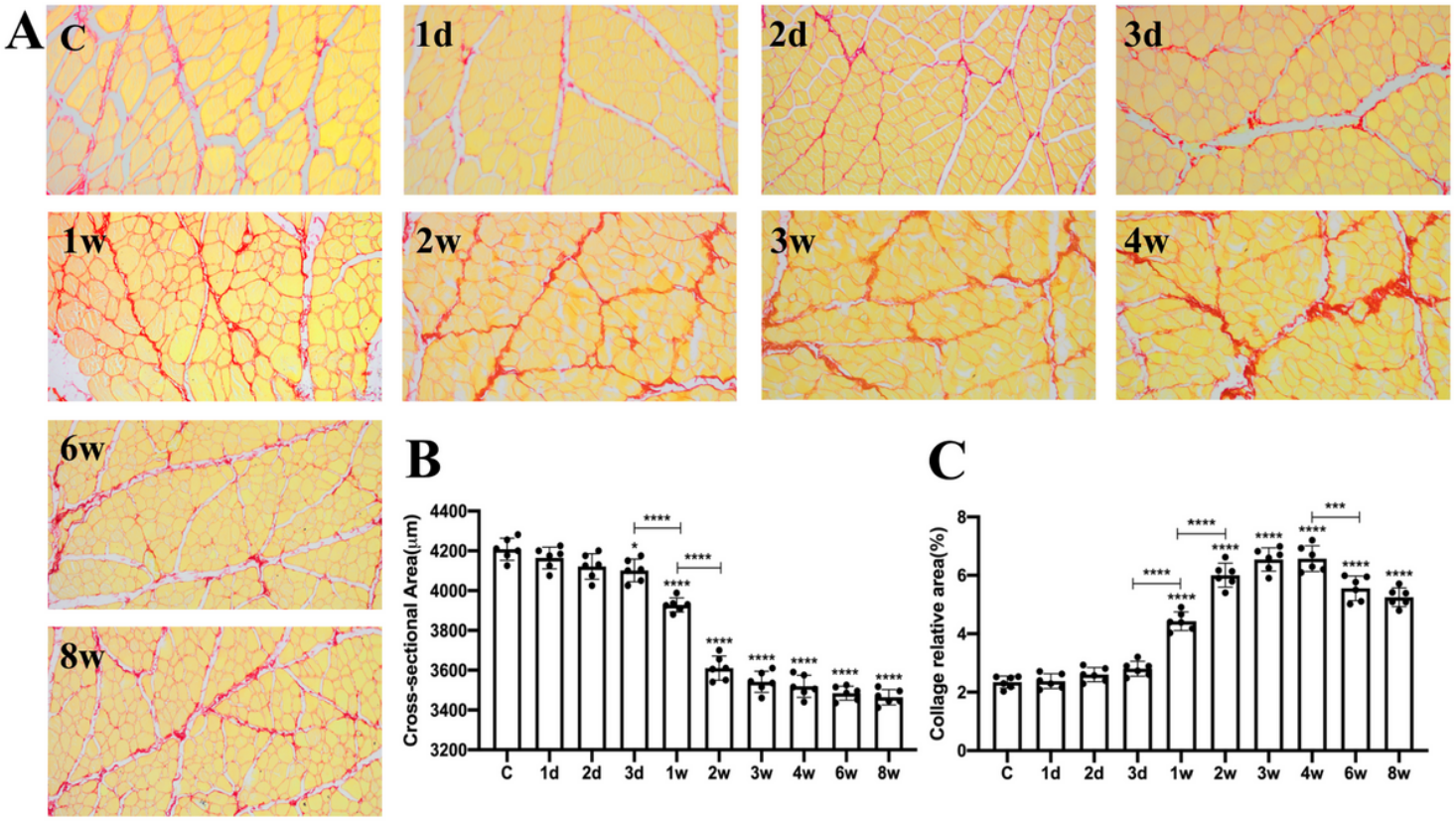

Figure 4

A: Morphological changes in the rectus femoris shown by Sirius red staining. B: Cross-sectional area of rectus femoris fibers after various periods of immobilization. C: Proportion of collagen deposition in the rectus femoris after various periods of immobilization. *P < 0.05; **P < 0.005; ***P < 0.0005; ****P < 0.0001. C, control group; 1d, immobilization-1d group; 2d, immobilization-2d group; 3d, immobilization-3d group; 1w, immobilization-1w group; 2w, immobilization-2w group; 3w, immobilization-3w group; 4w, immobilization-4w group; 6w, immobilization-6w group; 8w, immobilization-8w group.

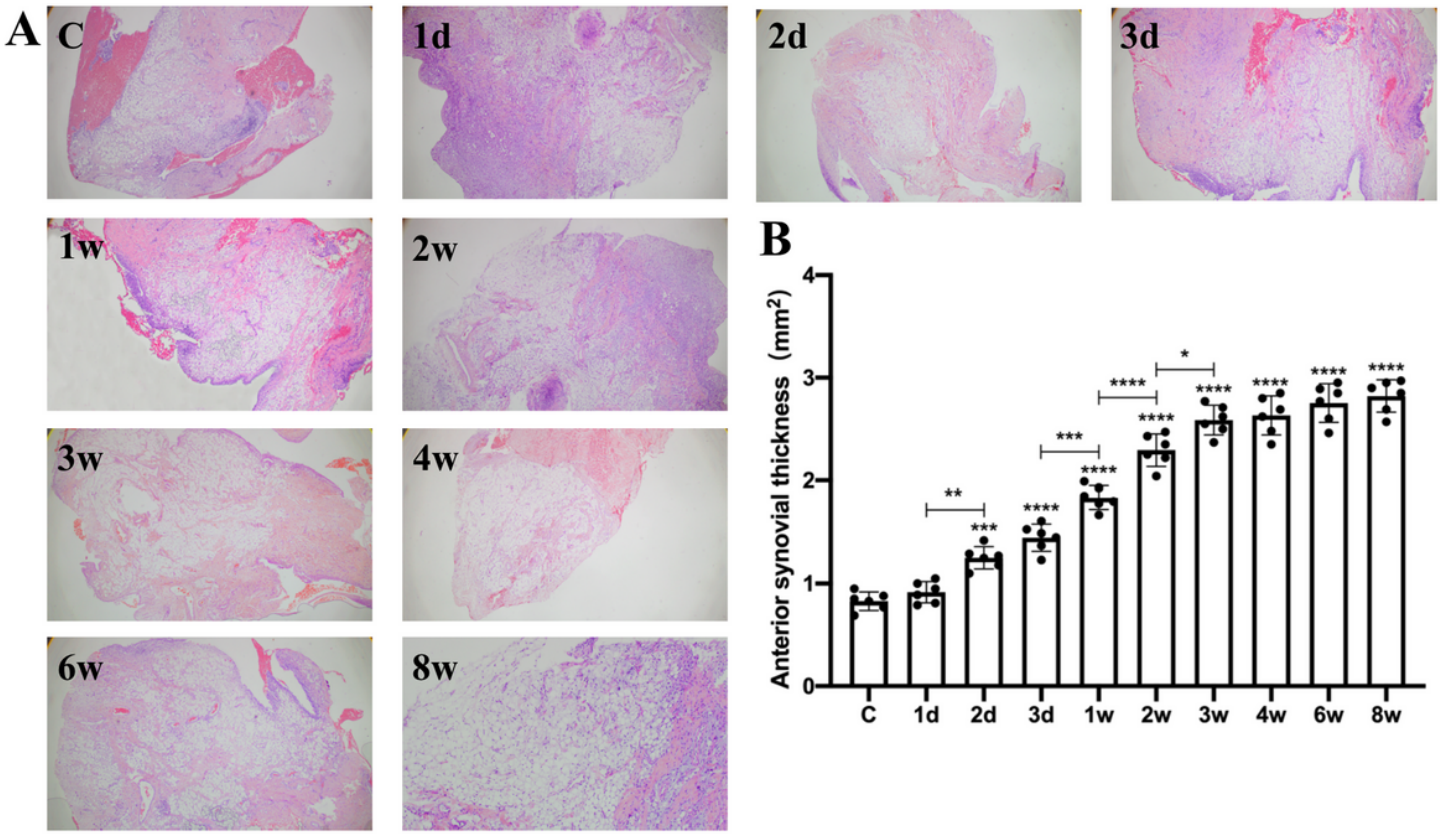

Figure 5

A: Morphological changes in the anterior joint capsule. B: Anterior joint capsule thickness. *P < 0.05; **P < 0.005; ***P < 0.0005; ****P < 0.0001. C, control group; 1d, immobilization-1d group; 2d, immobilization-2d group; 3d, immobilization-3d group; 1w, immobilization-1w group; 2w, immobilization-2w group; 3w, immobilization-3w group; 4w, immobilization-4w group; 6w, immobilization-6w group; 8w, immobilization-8w group.

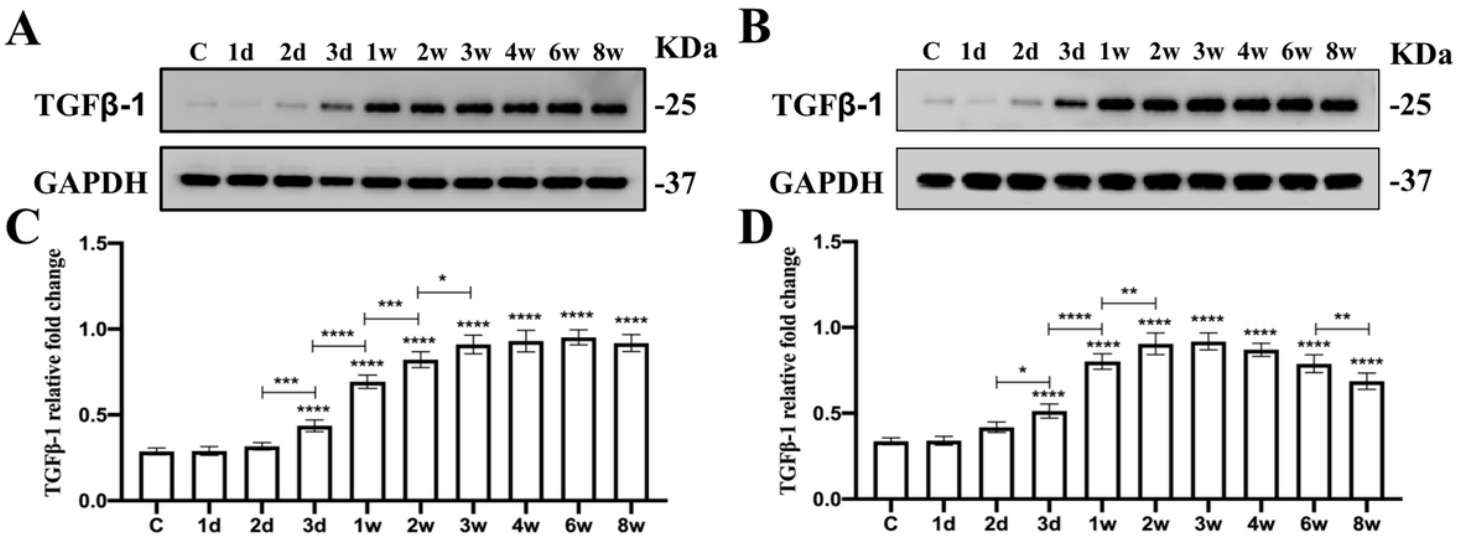

Figure 6

A: Changes in the intensities of the TGFβ-1 and GAPDH bands in the anterior joint capsule. B: Changes in the intensities of the TGFβ-1 and GAPDH bands in the quadriceps. C: Graphical representation of the expression level of TGFβ-1 relative to GAPDH in the anterior joint capsule. D: Graphical representation of the expression level of TGFβ-1 relative to GAPDH in the quadriceps. *P < 0.05; **P < 0.005; ***P < 0.0005; ****P < 0.0001. C, control group; 1d, immobilization-1d group; 2d, immobilization-2d group; 3d, immobilization-3d group; 1w, immobilization-1w group; 2w, immobilization-2w group; 3w, immobilization-3w group; 4w, immobilization-4w group; 6w, immobilization-6w group; 8w, immobilization-8w group.